~~RESTRICTED~~

Copy
RM L9H09

NACA

RESEARCH MEMORANDUM

PERFORMANCE CHARACTERISTICS OF TWO 6° AND TWO 12° DIFFUSERS AT HIGH FLOW RATES

By William J. Nelson and Eileen G. Popp

Langley Aeronautical Laboratory
Langley Air Force Base, Va.

NATIONAL ADVISORY COMMITTEE FOR AERONAUTICS

WASHINGTON

October 19, 1949

~~RESTRICTED~~

NACA RM L9H09

[redacted]

NATIONAL ADVISORY COMMITTEE FOR AERONAUTICS

RESEARCH MEMORANDUM

PERFORMANCE CHARACTERISTICS OF TWO 6° AND TWO 12° DIFFUSERS AT HIGH FLOW RATES

By William J. Nelson and Eileen G. Popp

SUMMARY

The aerodynamic characteristics of two circular-inlet and two annular-inlet diffusers of fixed-area ratio (1.75) have been determined over an operating range extending from an inlet Mach number of 0.2 to the choked condition. Pressure distributions across both the inlet and exit and along the diffuser walls are presented. Inlet-boundary-layer profiles were also measured.

The pressure-loss coefficient and diffuser effectiveness of each of these diffusers is shown to be essentially independent of Reynolds number in the subcritical-flow range; the performance falls off rapidly when sonic velocity is exceeded at any point in the system. Loss coefficients of the low-angle (6°) diffusers are shown to correlate readily with conical-diffuser data on a basis of wetted area; for the higher-angle (12°) diffusers the influence of wetted area is shown to be unimportant.

INTRODUCTION

The need for information concerning the performance of diffusers handling large quantities of air at high inlet velocities has become increasingly acute with the increasing speed of jet-propelled aircraft. The operational characteristics of the jet power plant require that the necessary air be inducted with the maximum possible pressure recovery and that uniform flow be delivered to the power plant. The bulk of the available data on diffuser performance has been obtained at relatively low values of Reynolds number and Mach number. Reference 1 presents diffuser characteristics based on the best of these data prior to 1944. Peters (reference 2) conducted some experiments on straight conical diffusers at a Reynolds number of 2×10^5 while Vedernikoff and Polzin (references 3 and 4) investigated two-dimensional diffusers of rectangular cross section at somewhat lower Reynolds numbers.

[redacted]

Naumann (reference 5) made a study of low-angle straight conical diffusers at Mach numbers apprcaching unity and Reynolds numbers up to 2×10^6. Bohm and Koppe (reference 6) dealt with a straight-wall diffuser of circular cross section having several different inner bodies at Reynolds numbers, based on hydraulic diameter, up to 1.4×10^5. In none of these references are data available on configurations applicable to turbojet installations where the air flow is delivered to the compressor through an annulus.

The present investigation was conducted in the induction aerodynamics laboratory of the Langley Aeronautical Laboratory during the summer of 1947 to provide information regarding the internal aerodynamic characteristics of diffusers of sufficient size and flow-handling capacity to be applicable to jet-power-plant installation at air flows comparable to those encountered with current jet engines.

To this end, four full-scale diffusers of equal expansion ratio (1.75) were investigated over a wide range of air flows. The diffusers investigated fall into two general types, one having circular inlet with annular exit sections and the other having annular cross-sections throughout. In each of these types, rates of area divergence corresponding approximately to those of 6° and 12° cones were investigated.

Data were recorded at air flows up to approximately 85 pounds per second. The corresponding Reynolds numbers based upon the hydraulic diameter of the inlet were 2×10^6 for the annular-inlet diffusers and and 6.0×10^6 for the circular-inlet diffusers. In each case the air-flow range was limited by choking of the diffuser.

SYMBOLS

H	boundary-layer-shape parameter (δ^*/θ)
$\bar{H}_i$	mass-weighted mean value of total pressure at diffuser entrance station
$\bar{H}_e$	mass-weighted mean value of total pressure at diffuser exit station
H_o	stream total pressure upstream of inlet
ΔH	total-pressure loss $\left(\bar{H}_i - \bar{H}_e\right)$

M_i mean entrance Mach number

p_x local wall static pressure

p_y local stream static pressure

u local velocity in boundary layer

u_o velocity at edge of boundary layer

w weight flow, pounds/second

η_D diffuser effectiveness

δ boundary-layer thickness

δ^* boundary-layer displacement thickness $\left[\int_0^\delta \left(1 - \frac{u}{u_o}\right) dy\right]$

θ boundary-layer momentum thickness $\left[\int_0^\delta \frac{u}{u_o}\left(1 - \frac{u}{u_o}\right) dy\right]$

APPARATUS AND METHODS

The general arrangement of the test setup used in this investigation is shown in figure 1. Air supplied by a 1000-horsepower centrifugal blower passed through a 16-mesh settling screen to a nozzle with an area reduction of 9:1. The test diffuser was attached directly to the nozzle and was followed by a constant-area tail pipe and a supplementary diffuser to reduce the discharge losses.

In figure 2 the area variation along these diffusers is compared with that of 6° and 12° conical diffusers. All areas were based on cross sections normal to the estimated mean-flow line. The cross-sectional area, thus defined, shows a sharp contraction following the initial expansion near the entrance of the circular-inlet diffusers. This contraction results from the use of a blunt inner body close to the entrance and the avoidance of abrupt curvature in the outer surface.

The diffusers were of metal construction throughout, with the exception of the inner body of the circular-entrance diffusers which were of laminated mahogany. Construction tolerances of ±1/32 of an inch were maintained on all dimensions with no abrupt discontinuities of the surface. The inner bodies of both diffusers were supported in the outer duct by means of streamline struts of thickness ratio 0.06. A smooth surface was obtained by repeated filling, painting, and sanding.

Fixed instrumentation consisted of four axial rows of static orifices mounted flush with the surface in both the outer duct wall and inner body with supplementary orifices installed at the inlet and exit cross sections and eight total-pressure rakes installed around the diffuser exit annulus with a reference total-pressure tube and stagnation thermocouple located approximately one diameter downstream of the settling screen. Simultaneous measurements of all fixed instrumentation were obtained by photographic recording of multiple-tube manometers. Radially movable pitot-static tubes were installed in the inlet at 90° intervals for the entrance surveys.

Preliminary explorations were made of diffuser entrance and exit flow conditions to establish proper techniques for making the subsequent measurements. Yaw surveys across the entrance of the circular-entrance diffuser established the fact that the maximum stream divergence from the center line was less than 7°, at which angle the error due to axial alinement of instrumentation was considered negligible. Preliminary static-pressure surveys across the diffuser exit annulus showed a straight-line variation from one wall to the other; therefore, a linear interpolation between the wall static pressures was used in the calculations presented herein. Further surveys with a rake of total-pressure tubes indicated that the wakes from the inner-body support struts did not spread to the fixed exit rakes.

Measurements of total and static pressures over the diffuser-entrance cross section were made over a range of air flows ranging up to and including the choking flow. All total-pressure measurements were referenced to the total pressure in the supply duct ahead of the diffuser entrance approach contraction, and all static-pressure measurements were referenced to a single wall static pressure taken at the diffuser entrance station. The entrance rakes were removed during tests in which the longitudinal wall static pressures and/or total pressures in the exit cross section were being recorded. Pressures in these tests were referenced in the same way as in the inlet surveys. Weight flow was determined by first calibrating the entrance in terms of the ratio of entrance reference wall static pressure to upstream reference total pressure by extensive pressure surveys across the inlet. Mean entrance Mach number was computed from the weight flow, the entrance

area, and the upstream stagnation conditions following the method of reference 7. Moisture condensation was avoided by recirculation of the air to the blowers, thus elevating the temperature to exceed saturation temperature at all points in the system. The temperature was controlled by varying the proportion of the recirculated air.

RESULTS AND DISCUSSION

Performance.- Performance of the four diffusers investigated in the current research is discussed first on a basis of the loss in total pressure experienced by the air in flowing through the diffuser and second in terms of the increase in static pressure effected by the compression. It is apparent that these two characteristics are related, although the relative performance of different diffusers will not necessarily be the same on both bases.

The loss in stagnation pressure, expressed as a coefficient $(\Delta H/q_i)$, is presented in figure 3 as a function of mean inlet Mach number (M_i) for each of the four diffusers tested. The values of M_i were determined from the mass-flow rate and the stream stagnation conditions. The loss coefficient in each case was essentially independent of mean inlet Mach number below a certain critical value which will be shown later to correspond to the occurrence of sonic velocities in the vicinity of the inlet.

Increasing the pressure difference across the system beyond that required to reach the critical flow produces further losses with no increase in the value of the mean inlet Mach number. In the subcritical-flow range, higher losses were measured with the 6° diffusers than in those with 12° expansion. This is contrary to the results of numerous tests in conical diffusers with thick inlet boundary layers (see reference 1). The measured losses $\Delta H/q_i$ of 0.042 and 0.040 in the 12° diffusers of circular and annular inlet, respectively, are in excellent agreement with the corresponding value of 0.040 for conical diffusers at low Reynolds number from reference 1. The loss coefficient of 0.024 (reference 1) for a 6° conical diffuser, however, is lower than those measured in these tests, 0.050 for the circular-inlet configuration and 0.066 for the annular inlet, by factors closely approximating the ratio of wetted areas. This latter fact suggests the possibility of coordinating low-angle-diffuser data on a basis of the length-to-mean-hydraulic-diameter ratio, as in pipe flow, since the major source of pressure loss in such diffusers is in wall friction. The performance of large-angle diffusers, on the other hand, is influenced largely by flow separation and therefore would not be expected to correlate on this basis.

If, as previously stated, the critical flow is associated with the occurrence of sonic velocity in the vicinity of the inlet, it might be expected that the shorter diffusers, because of their greater curvature near the inlet, would have lower critical flows than the 6° diffusers. This difference was observed with both configurations. It is also noted that the critical flow was appreciably lower for the circular inlets than for the annular ones. Although the inlet cross-sectional area was the same for all these diffusers, the effective area of the circular-inlet configurations is appreciably lower than that of the annular-inlet diffuser because of the obstruction to flow caused by the presence of an inner body directly behind these inlets. The effective area is probably the predominant factor in determining the critical air flows. The very low critical flow of the 12° circular-inlet diffuser is probably also influenced by the 5-percent area constriction downstream of the inlet, figure 2.

In the supercritical-flow range the rapid rise in total-pressure loss is caused by increased normal-shock loss and shock-induced-separation loss. Shadowgraphs of boundary-layer behavior in the presence of compression shock, together with detailed pressure surveys, in the vicinity of a curved surface, are presented in reference 8.

The pressure-loss data are also presented in figure 4 plotted against weight flow rate. Plotted in this manner, the curves rise less steeply in the supercritical region because the increase in stagnation pressure increases the density and therefore the weight flow, although the mean inlet Mach number remains constant.

The static-pressure rise effected by the diffusers is presented in figures 5 and 6 in terms of the rise which would have been effected under ideal conditions, that is, uniform velocity over the duct cross section at both inlet and exit and no loss in stagnation pressure between the inlet and exit. The diffuser effectiveness, thus defined, is nearly constant throughout the subcritical range of these tests, decreasing abruptly at supercritical flows. Similar characteristics have been observed in references 3 and 4. Direct quantitative correlation of these data, however, has not been obtained. Of the circular-inlet configurations, the 12° diffuser has a slightly higher effectiveness in the subcritical range but reaches the critical flow at a lower mean inlet Mach number. As has been pointed out earlier the critical flow of this diffuser is influenced markedly by the flow obstruction caused by the inner body and the contraction behind the inlet. The subcritical effectiveness of the annular inlets was approximately the same for both diffusers, although the pressure-loss data showed 50 percent more loss with the 6° diffuser than for the 12° system. That these results are not contradictory is apparent if one realizes that the diffuser effectiveness is influenced by both the magnitude and distribution of the total pressure at the inlet and exit. A change in distribution without changing the absolute value of the total pressure would

therefore change the effectiveness without influencing the loss coefficient. The over-all performance of the annular-inlet diffuser is slightly superior to the circular-inlet designs investigated. The rapid decrease in effectiveness in the supercritical regime is associated with the increased total-pressure losses and the reduction in effective area at the exit resulting from flow separation behind the compression shocks near the entrance.

These data are also plotted against weight flow rate, figure 6, to facilitate study in the region above the critical flow.

Inlet distribution.- Previous research, notably that of Peters, reference 2, has shown that diffuser performance varies considerably with changes in velocity distribution across the inlet. In general, it is shown that pressure recovery deteriorates with thickening of the inlet boundary layer; it is necessary, therefore, to regard diffuser performance as inextricably associated with the inlet-boundary-layer profiles although no quantitative relationships have been established. Typical inlet-boundary-layer profiles are presented for both the circular and the annular inlets for several different air flows in figure 7. No control was exercised over the inlet profiles in these tests and no attempt has been made to isolate the effect of inlet-boundary-layer profile.

Outside the boundary layer the total pressure was uniform over both the annular and circular inlets; the static pressure, however, showed marked variations. (See figs. 8(a) and 8(b).) At the circular inlet the static pressure was low near the outer walls and increased regularly to values approaching the total pressure at the center line. This is to be expected in any inlet which is followed by a large obstruction originating very close to the inlet. Similar profiles were obtained with the longer inlet but the pressure gradients involved were much smaller because of the greater fineness ratio of the inner body and the greater distance between the inlet station and the front of the inner body. The air approaching the obstruction at subsonic velocities slows down at a considerable distance ahead of the body, thus forcing the entering air to flow with increasing velocity near the outer wall. Slight curvature of the wall surface therefore produces local supersonic flow followed by a compression shock at relatively low flow rates. Although the annular-inlet passage was unobstructed downstream, local wall curvature along the inner body produced effects along this wall similar to those observed with the circular-inlet system, but supersonic velocities were delayed to somewhat higher flow rates.

Wall static-pressure gradient.- The development of the boundary layer and the occurrence of flow separation are closely associated with the static-pressure gradient along the diffuser as well as with the

entrance conditions. The wall static pressure p_x/H_o along each diffuser is shown in figure 9 for several representative flow rates. These data show marked differences in pressure gradient along the inner and outer wall indicating that local wall curvature is of considerable importance in establishing the static-pressure distribution along the diffuser wall. The differences are most marked near the entrance of the circular inlet where high curvature near the inlet produces very low pressures along the outer wall while stream total pressure is recorded at the nose of the central body. The pressure-distribution characteristics along the walls of the annular diffusers are in good agreement with the characteristics of the circular-inlet diffusers.

The occurrence of sonic velocities, $\frac{p}{H} = 0.528$, will be observed to correspond closely to the critical flows previously noted in the performance characteristics of these diffusers.

Exit total-pressure distribution.- Total pressures were measured along eight radii at the exit station of each diffuser. Typical data from the 12° diffusers are presented in figure 10 for several values of inlet Mach number. At low velocities the losses were very small and concentrated at the walls with approximately equal loss along the inner and outer wall. The loss increased regularly with inlet Mach number until the critical flow was reached, at which point the loss behind the circular inlet increased abruptly along the inner wall. Behind the annular inlet, however, the systematic progression was maintained even through the critical range. For both diffusers in the subcritical region, the flow in the exit annulus is quite symmetrical and appears to be free from flow reversal.

CONCLUSIONS

From this investigation of the performance characteristics of two 6° and two 12° diffusers it is concluded that:

1. Diffuser loss coefficient and effectiveness are essentially independent of Reynolds number at subcritical flow rates.

2. The loss coefficient of the low-angle diffusers at subcritical flows correlates readily with available conical-diffuser data on a basis of wetted area.

3. At subcritical air flows the loss coefficient of the 12° annular diffusers is less than that of the corresponding 6° diffusers.

4. Diffuser performance falls off rapidly when sonic velocity is exceeded at any point along duct walls because of losses resulting from compression shock and shock-induced separation.

5. The critical flow rate for these circular-inlet diffusers is lower than that for these annular-inlet diffusers because of the higher rate of curvature near the inlet, smaller effective inlet area, and, in the 12° diffuser, an area contraction which occurred behind the inlet.

6. The total-pressure distribution around the exit annulus of all these diffusers is very uniform throughout the subcritical flow range with but small irregularities below the highest flow rates attained.

Langley Aeronautical Laboratory
National Advisory Committee for Aeronautics
Langley Air Force Base, Va.

REFERENCES

1. Henry, John R.: Design of Power-Plant Installations. Pressure-Loss Characteristics of Duct Components. NACA ARR L4F26, 1944.

2. Peters, H.: Conversion of Energy in Cross-Sectional Divergences under Different Conditions of Inflow. NACA TM 737, 1934.

3. Vedernikoff, A. N.: An Experimental Investigation of the Flow of Air in a Flat Broadening Channel. NACA TM 1059, 1944.

4. Polzin, J.: Flow Investigations in a Two-Dimensional Diffuser. R.T.P. Translation No. 1286, British Ministry of Aircraft Production. (From Ingenieur-Archiv, vol. XI, no. 5, Oct. 1940, pp. 361-385).

5. Naumann: Wirkungsgrad von Diffusoren bei hohen Unterschallgeschwindigkeiten. FB Nr. 1705, Deutsche Luftfahrtforschung (Berlin-Adlershof), 1942.

6. Bohm, H., and Koppe, M.: The Influence of Friction on Steady Diffuser Flows at High Speed. Joint Intelligence Objectives Agency, Washington, D. C., July 23, 1946.

7. Taylor, G. I., and Maccoll, J. W.: The Mechanics of Compressible Fluids. Steady Flow through Channels. Vol. III of Aerodynamic Theory, div. H., ch. II, sec. 3, W. F. Durand, ed., Julius Springer (Berlin), 1935, pp. 224-226.

8. Froessel, W.: Investigation of Compressible Flow on and near a Curved Profile. AAF Translation No. F-TS-1517-RE, Air Materiel Command, Wright Field, Dayton, Ohio, Aug. 1947.

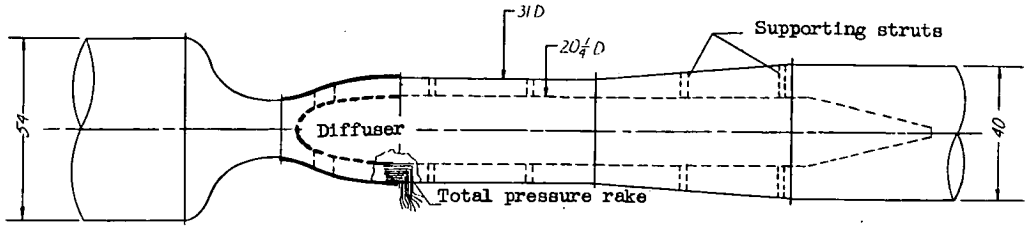

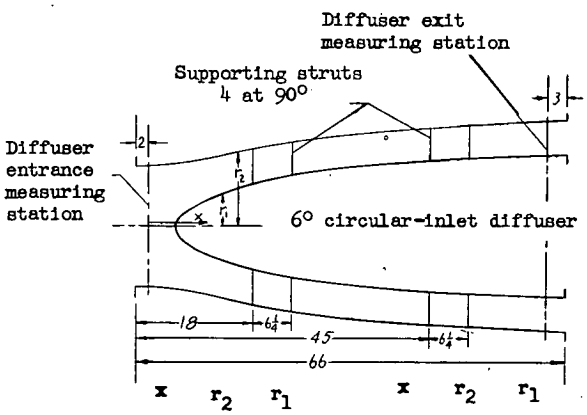

x	r_2	r_1	x	r_2	r_1
0	8.89	—	32	13.31	8.59
2	8.89	—	36	13.73	8.94
4	9.05	—	40	14.10	9.24
6	9.24	0	44	14.42	9.49
8	9.50	2.12	48	14.70	9.69
10	9.83	3.41	52	14.98	9.85
12	10.22	4.42	56	15.20	9.99
16	11.04	5.76	60	15.40	10.08
20	11.80	6.78	64	15.50	10.13
24	12.39	7.57	66	15.50	10.13
28	12.88	8.15			

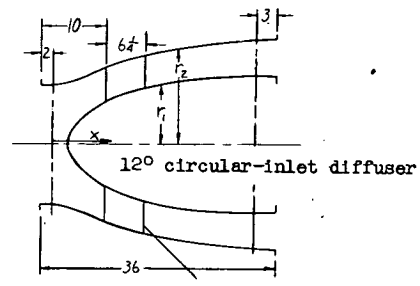

x	r_2	r_1	x	r_2	r_1
0	8.89	—	20	13.88	9.07
2	8.89	—	22	14.23	9.33
4	9.20	0	24	14.54	9.54
6	9.83	3.48	26	14.83	9.74
8	10.65	5.20	28	15.10	9.92
10	11.42	6.30	30	15.32	10.03
12	12.10	7.10	32	15.50	10.10
14	12.64	7.76	34	15.50	10.13
16	13.10	8.34	36	15.50	10.13
18	13.50	8.74			

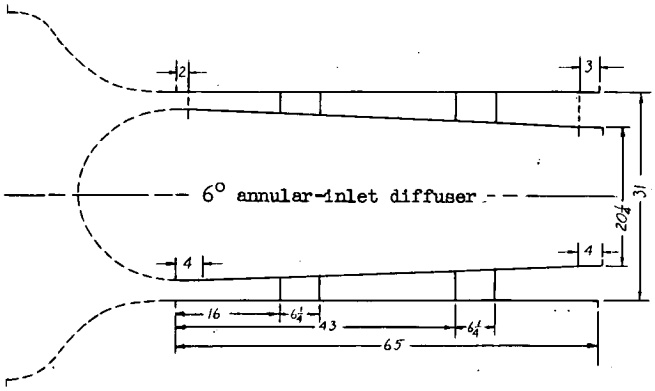

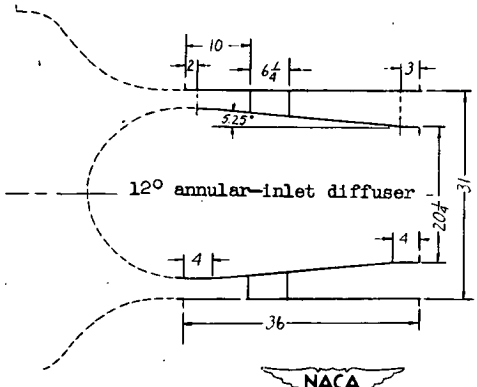

NOTE: All dimensions are in inches.

Figure 1.– Test apparatus.

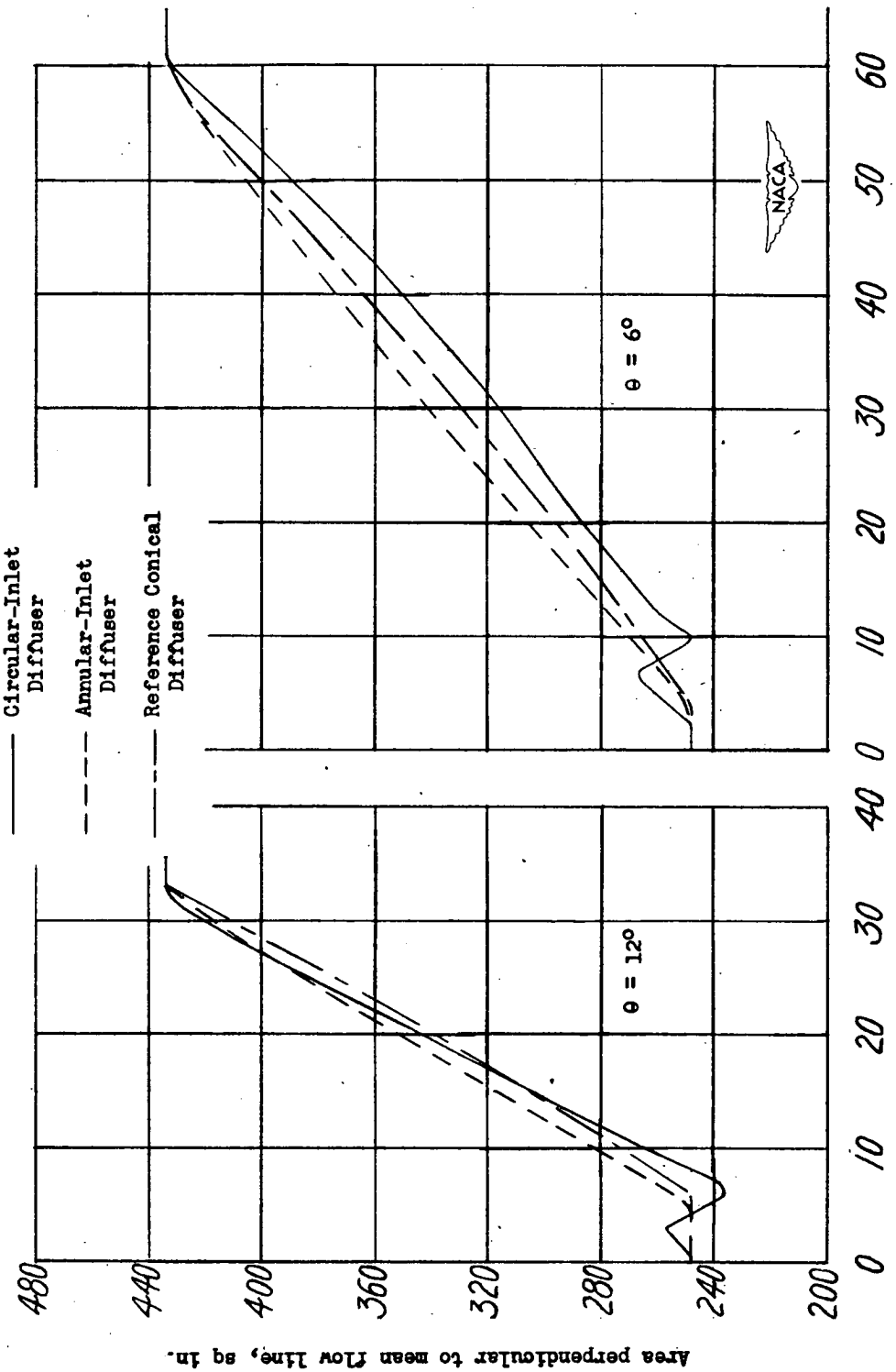

Figure 2.- Area distribution along diffuser.

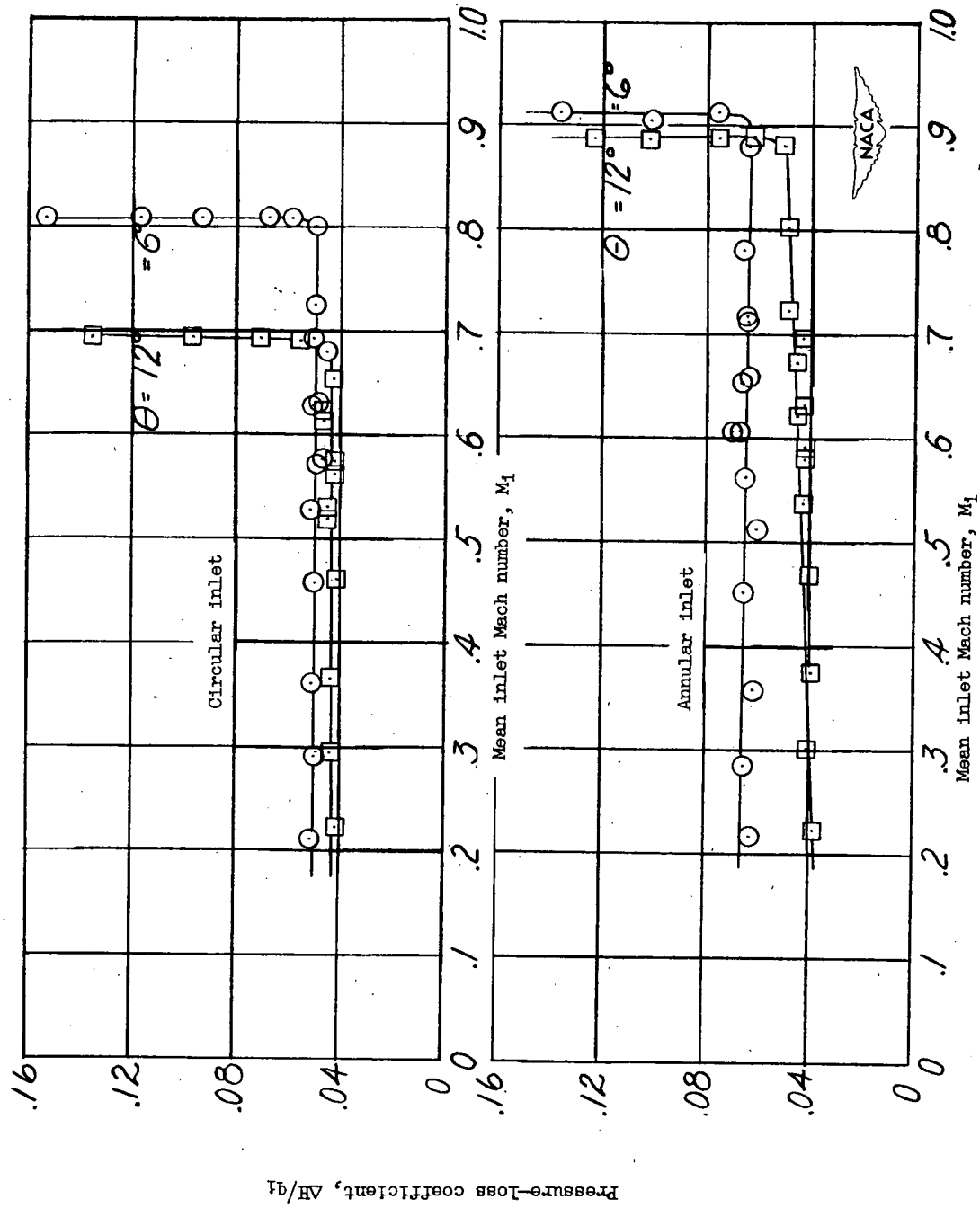

Figure 3.- Effect of mean inlet Mach number on pressure-loss coefficient.

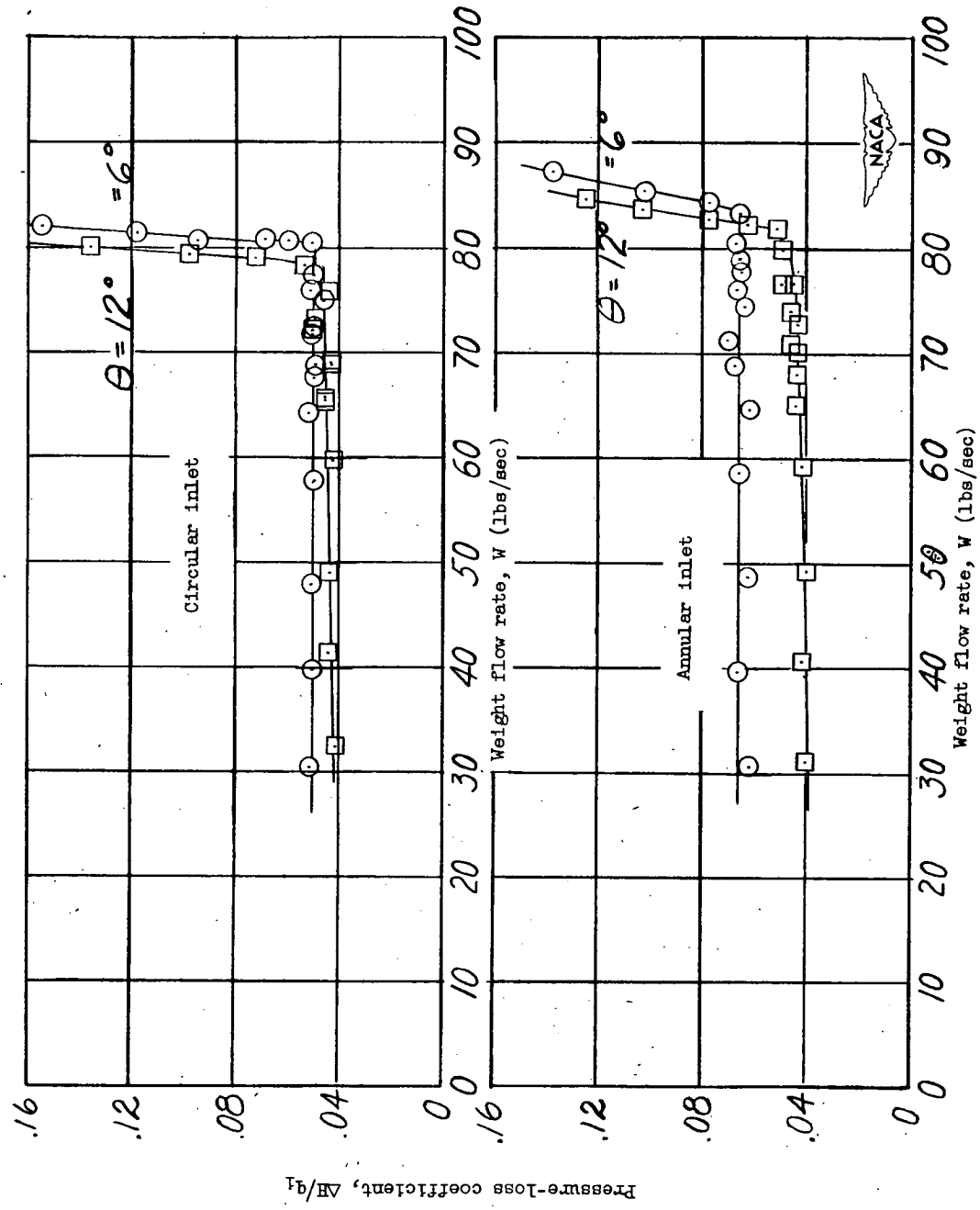

Figure 4.- Effect of weight flow rate on pressure-loss coefficient.

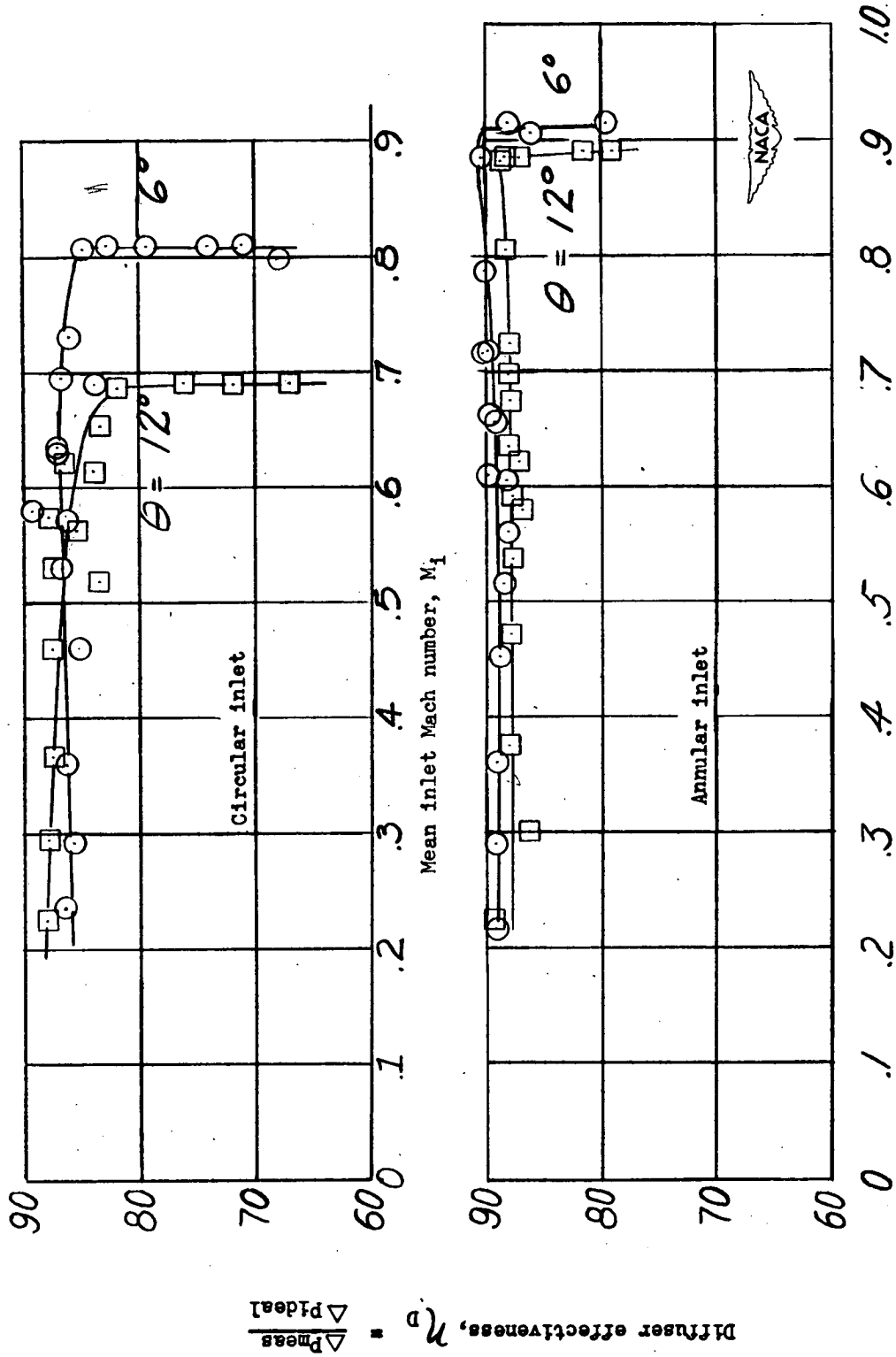

Figure 5.- Effect of mean inlet Mach number on diffuser effectiveness η_D.

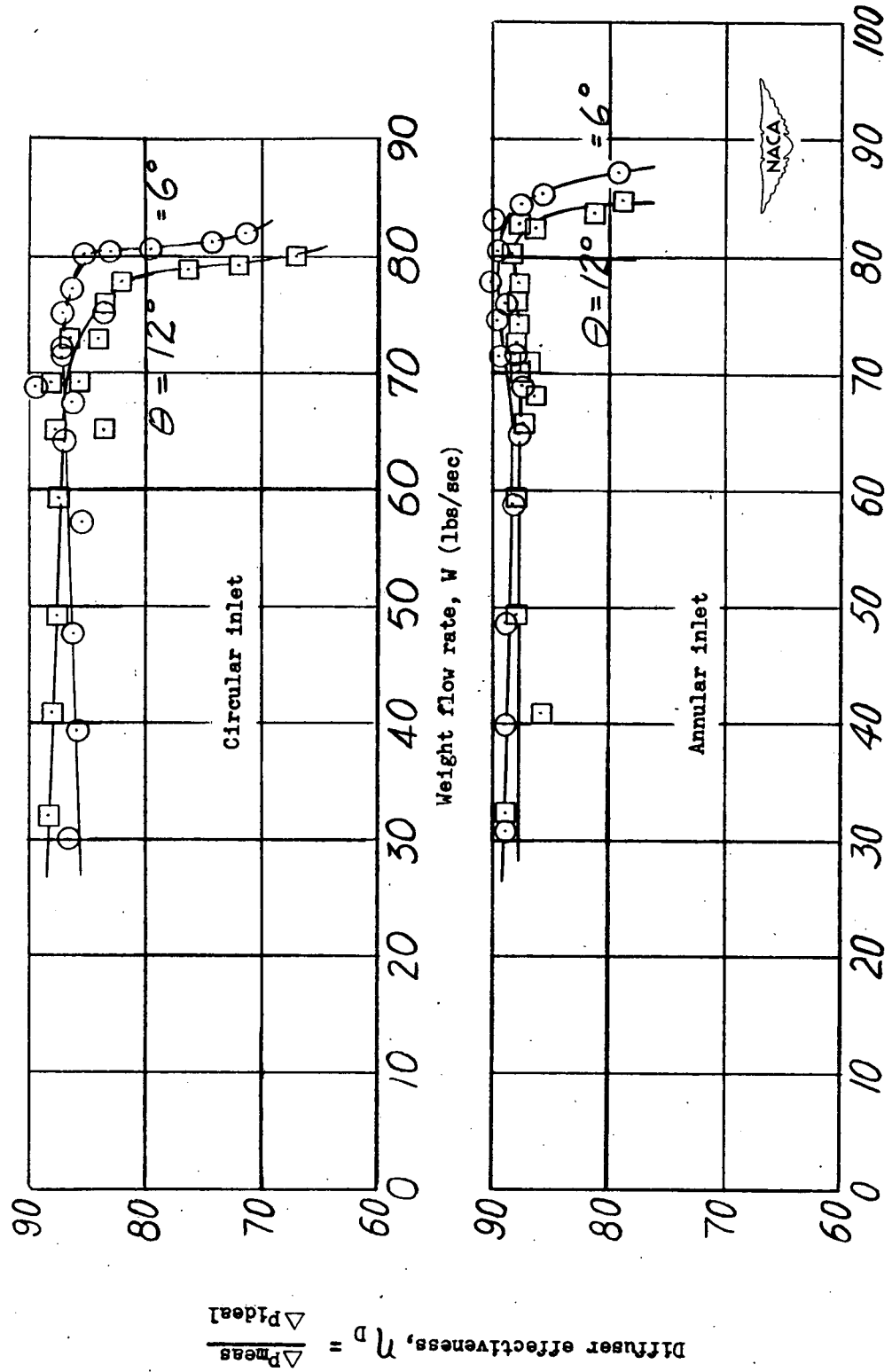

Figure 6.- Effect of internal flow on diffuser effectiveness η_D.

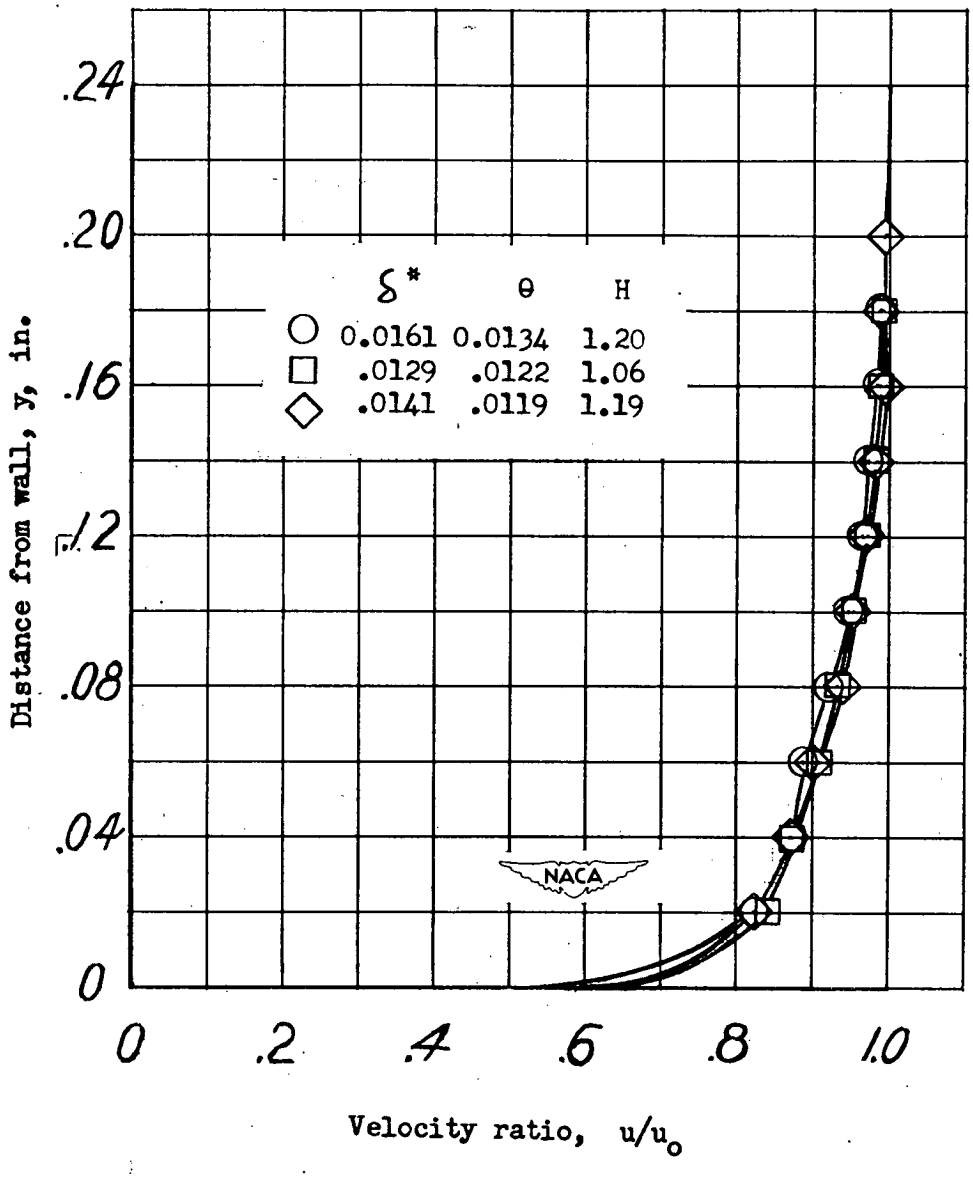

(a) Circular–inlet diffuser.

Figure 7.– Typical inlet boundary–layer profiles.

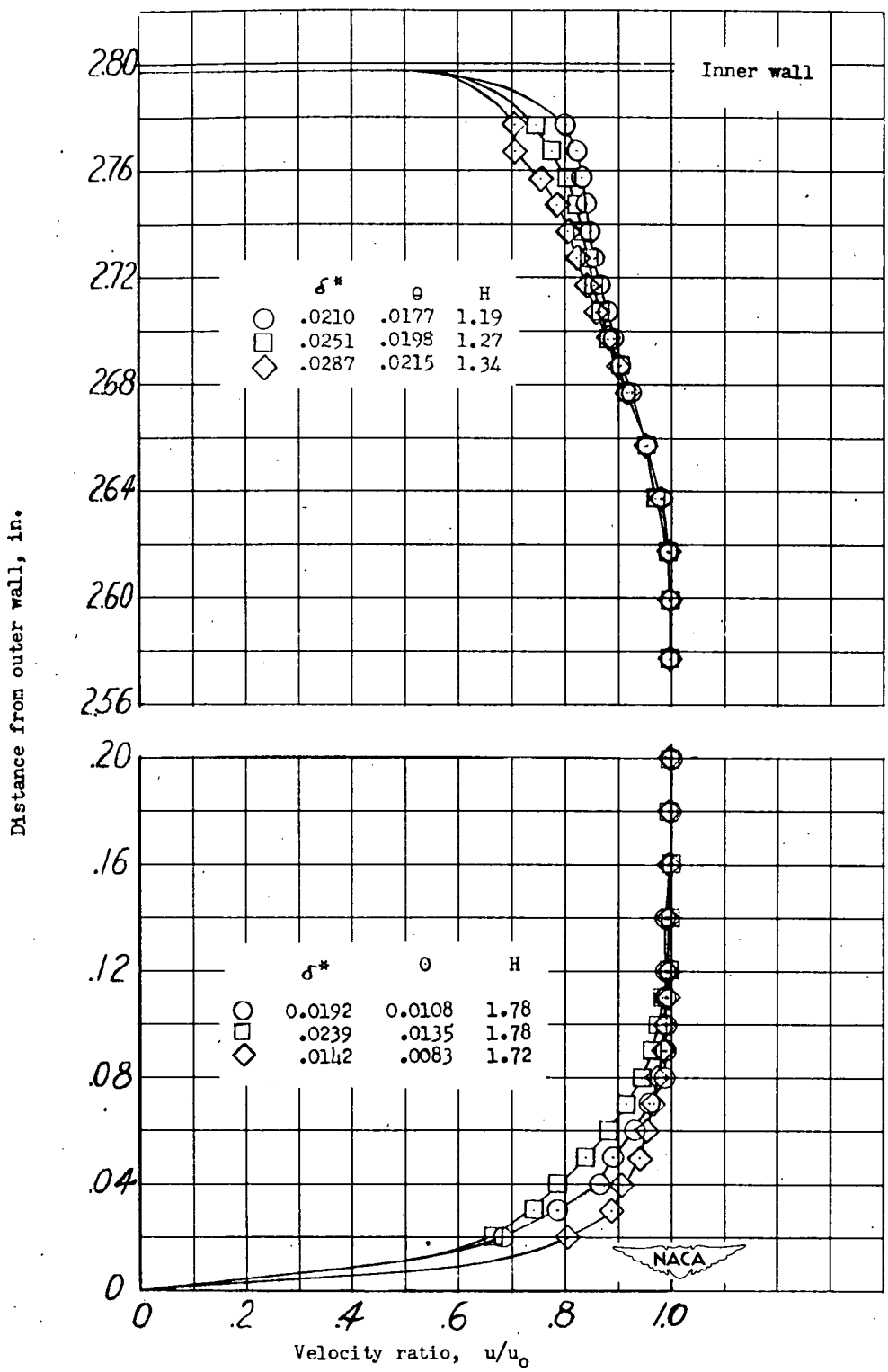

(b) Annular-inlet diffuser.

Figure 7.– Concluded.

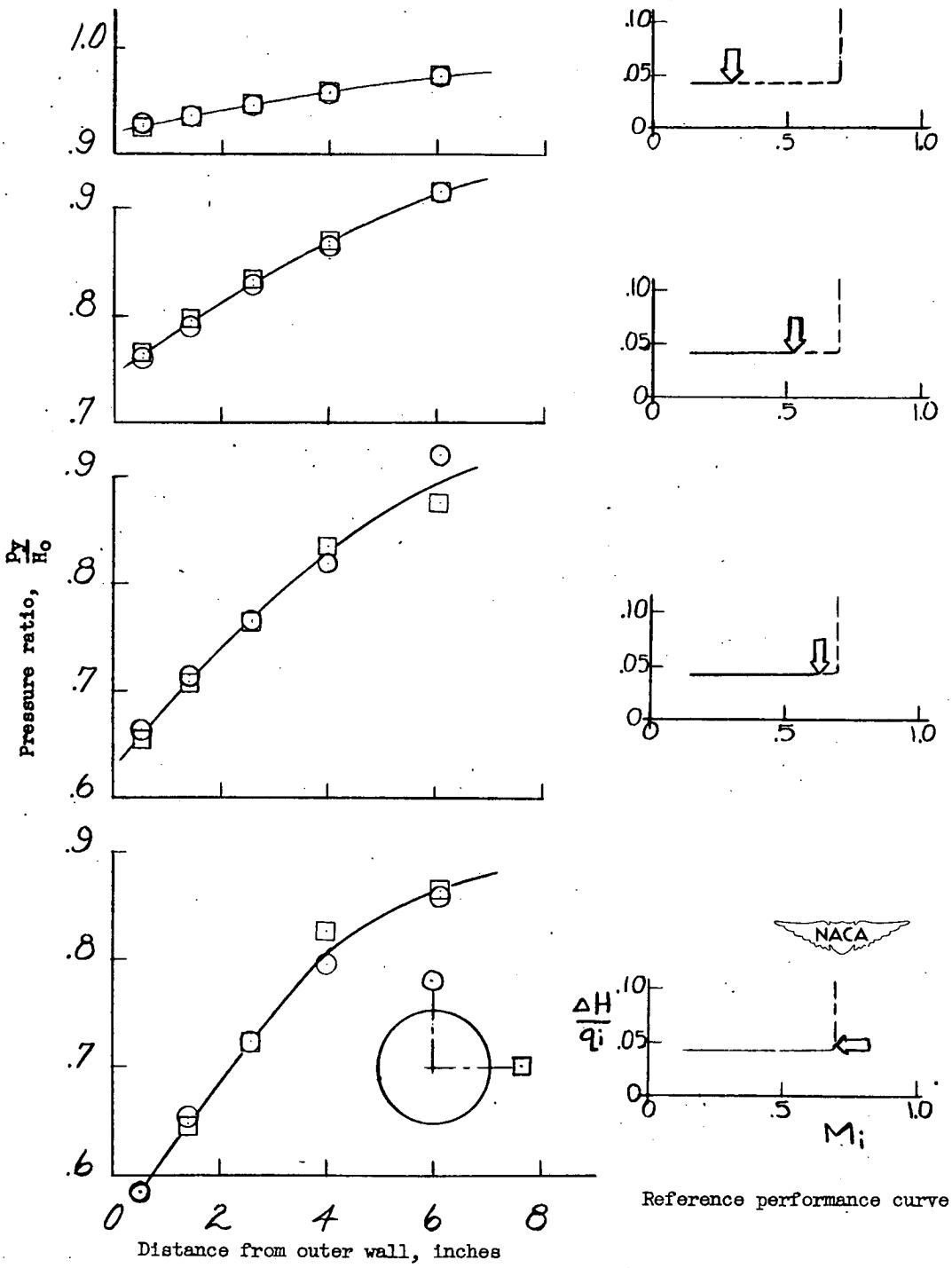

(a) Circular–inlet diffuser.

Figure 8.– Typical static–pressure distribution across the diffuser inlet.

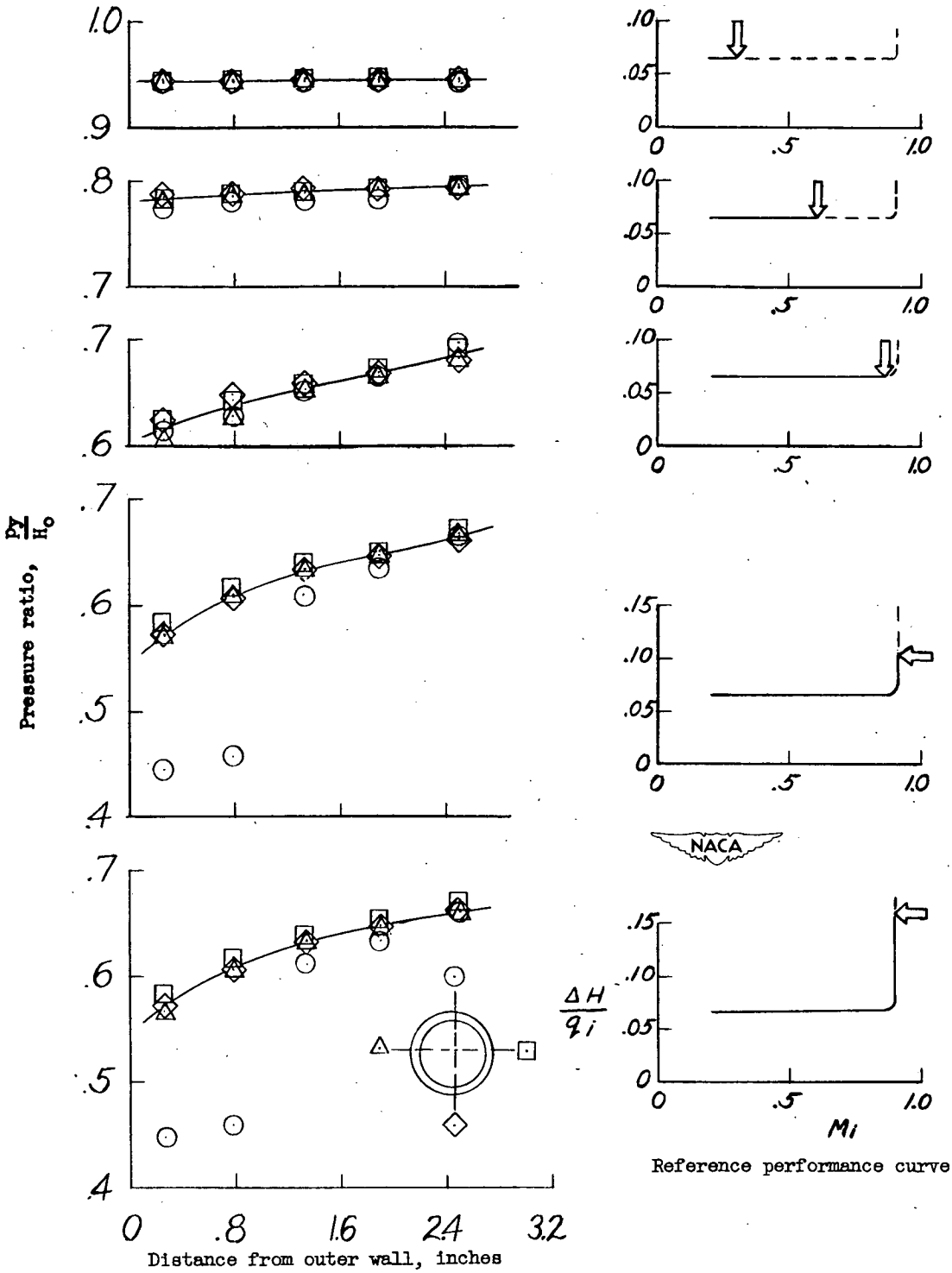

(b) Annular-inlet diffuser.

Figure 8.- Concluded.

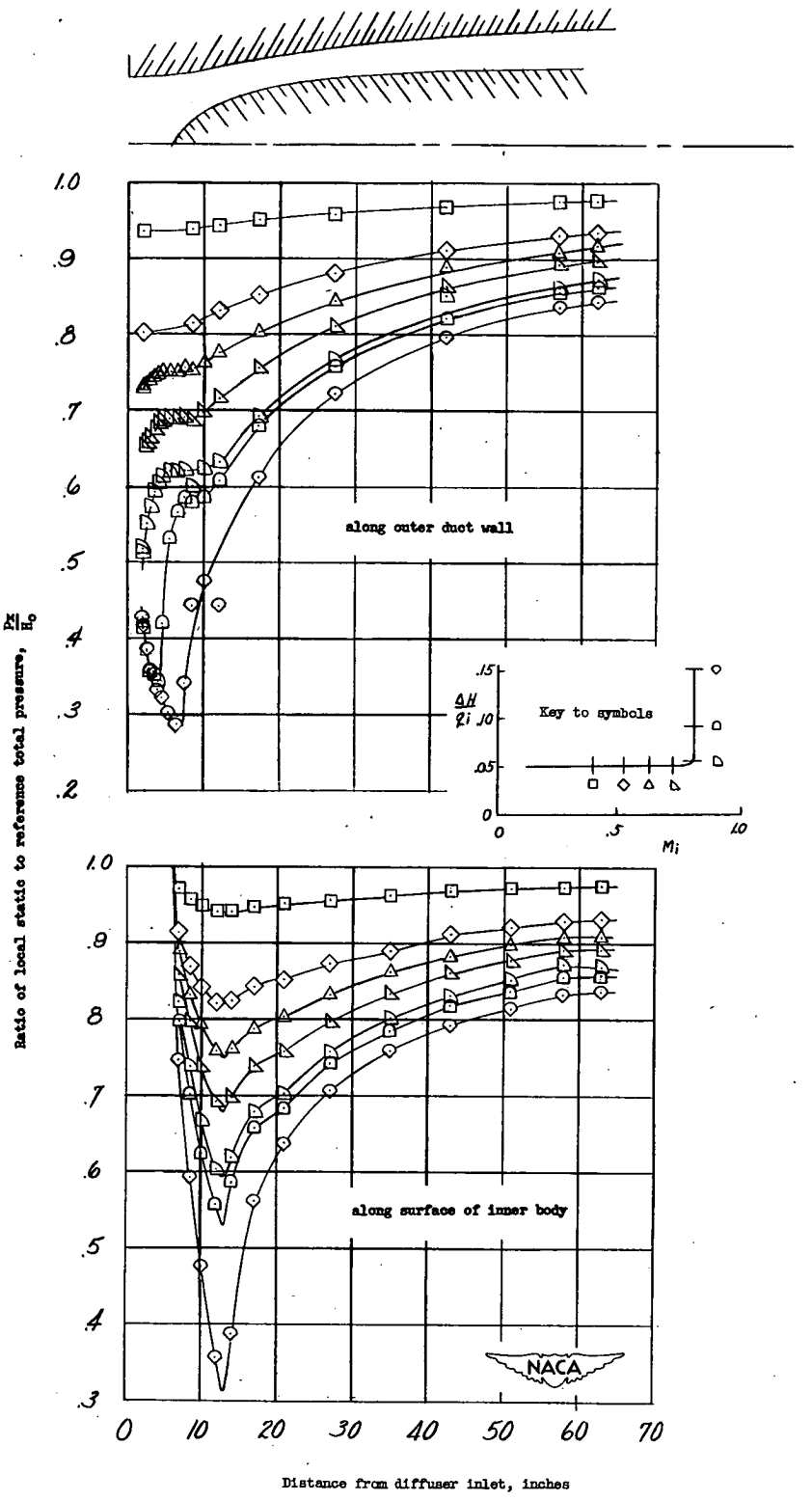

(a) 6° circular-inlet diffuser.

Figure 9.- Static-pressure distribution along the diffuser walls.

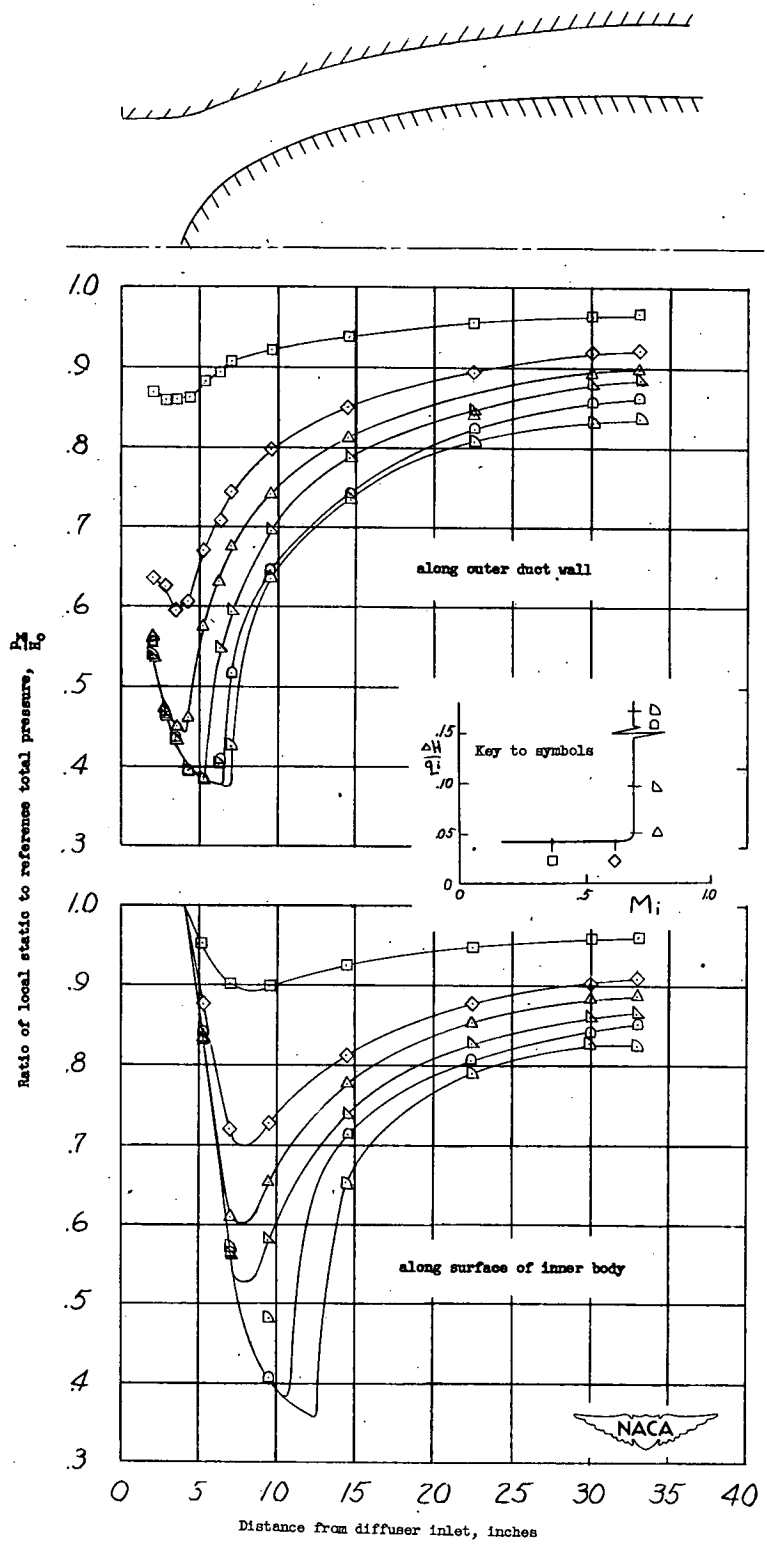

(b) 12° circular-inlet diffuser.

Figure 9.- Continued.

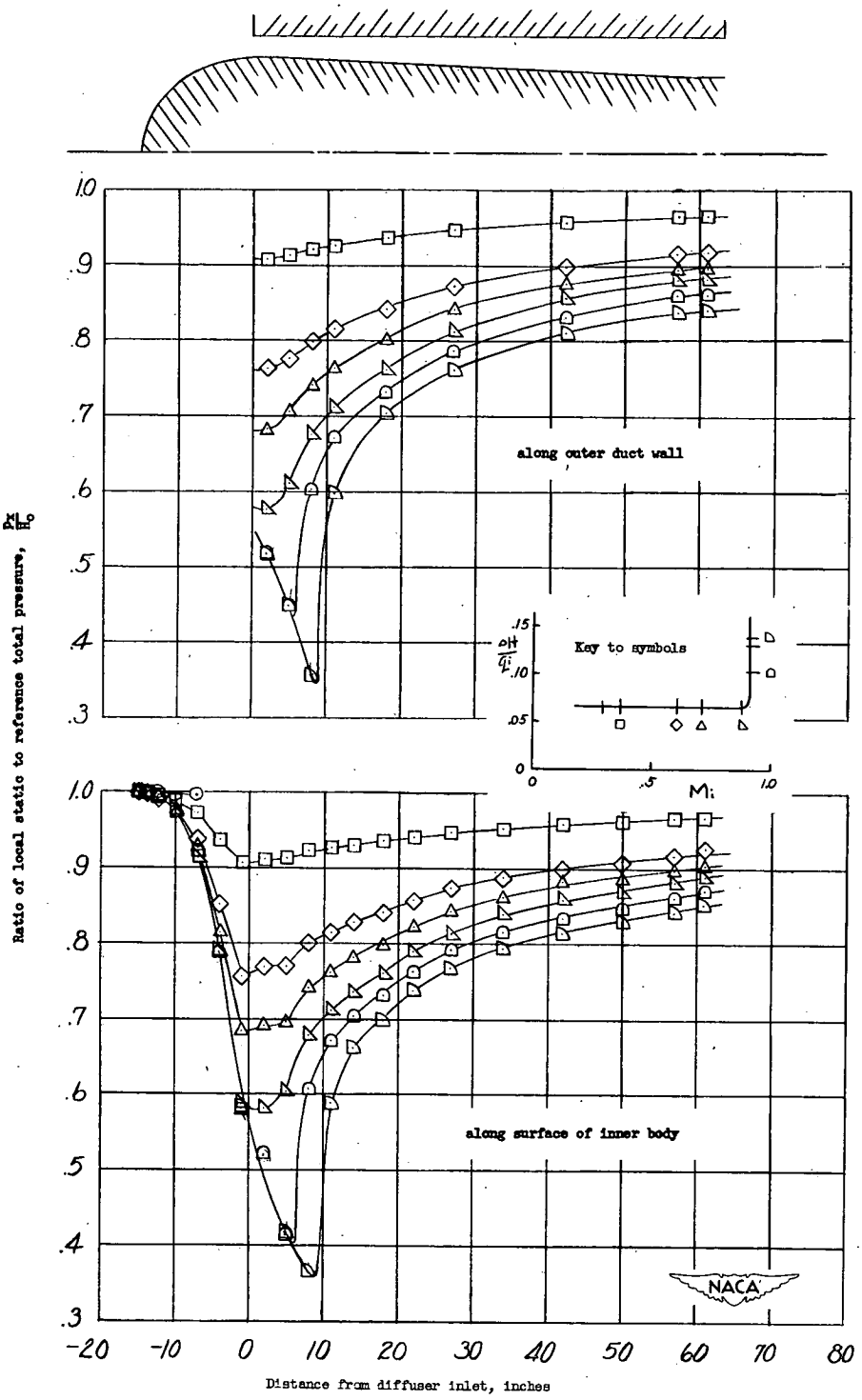

(c) 6° annular-inlet diffuser.

Figure 9.- Continued.

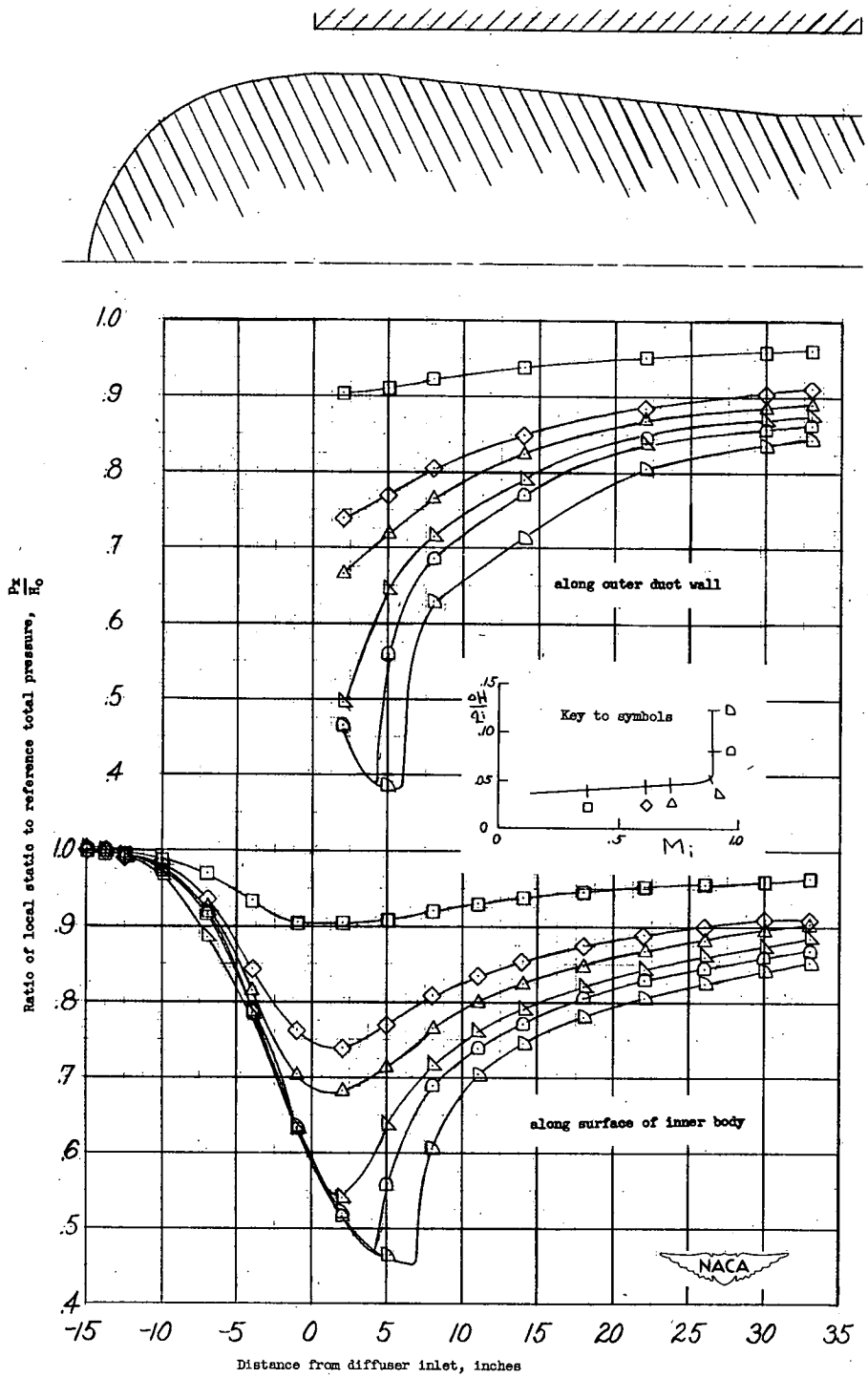

(d) 12° annular-inlet diffuser.

Figure 9.- Concluded.

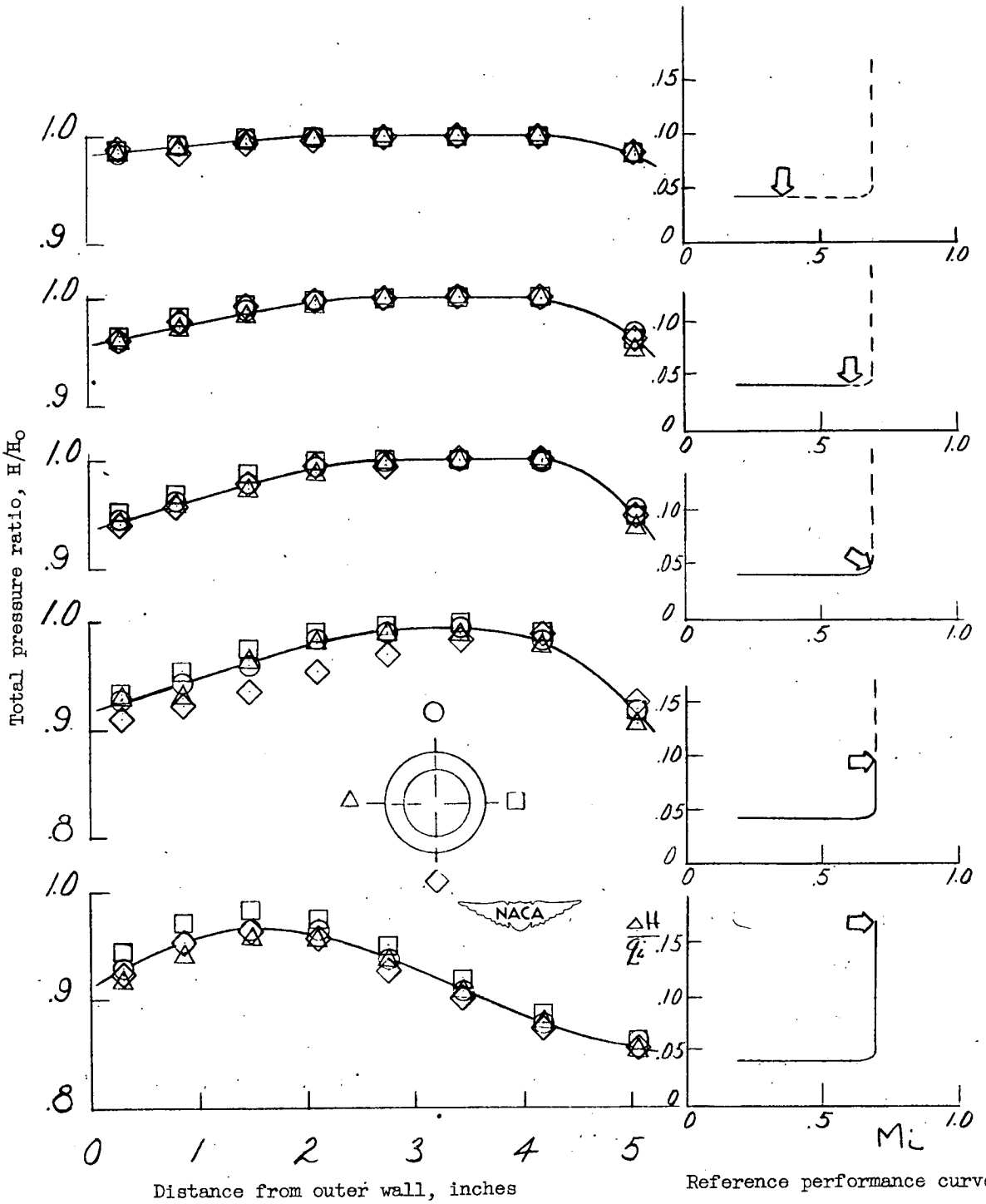

(a) Circular-inlet diffuser.

Figure 10.- Typical total pressure distribution across the diffuser exit.

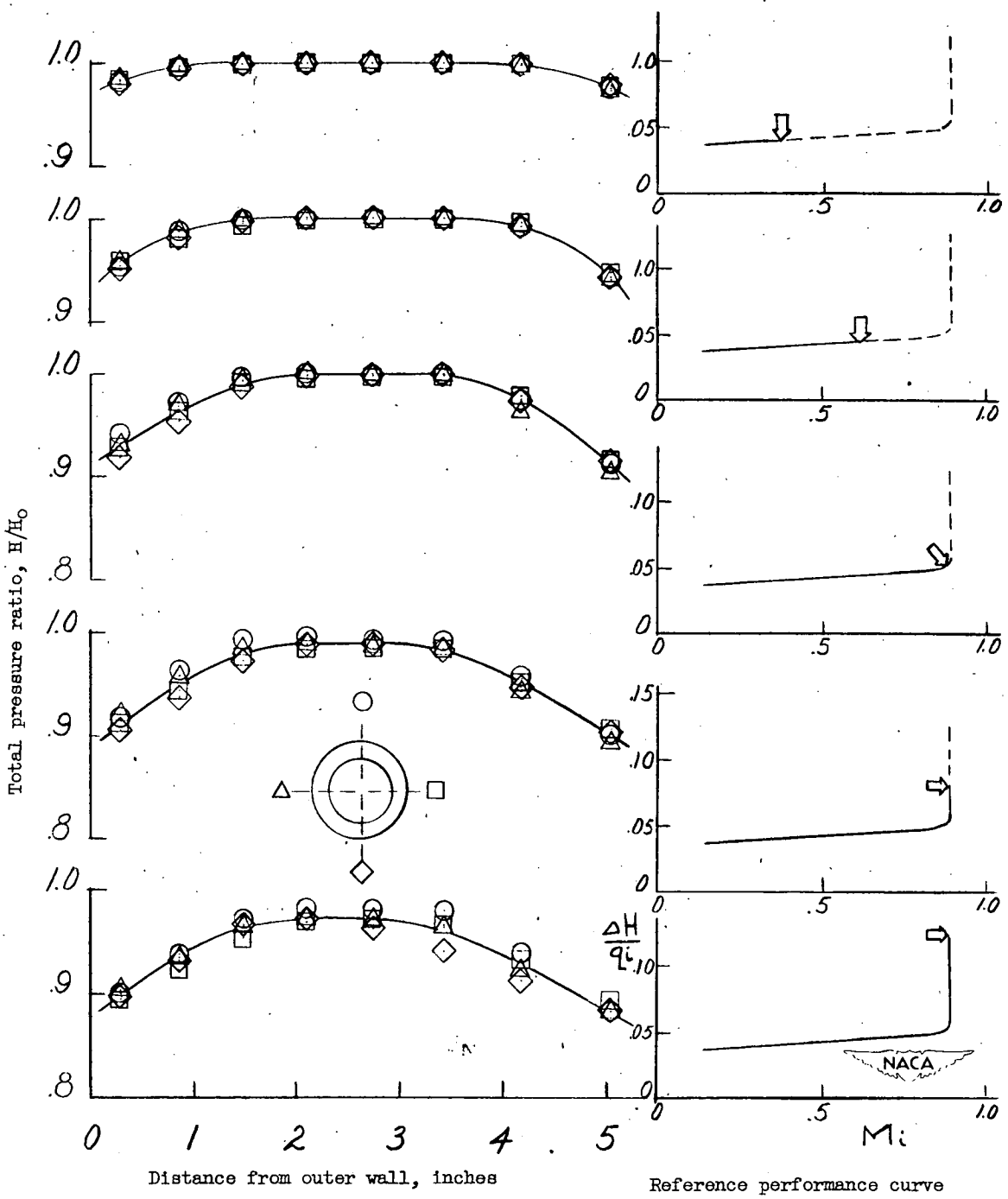

(b) Annular-inlet diffuser.

Figure 10.- Concluded.